Lawrence Berkeley National Laboratory
LBL Publications

Title

The Influence of ENSO Diversity on Future Atlantic Tropical Cyclone Activity

Permalink

https://escholarship.org/uc/item/2hw4v657

Journal

Journal of Climate, 37(15)

ISSN

0894-8755

Authors

Mueller, Teryn J

Patricola, Christina M

Bercos-Hickey, Emily

Publication Date

2024-08-01

DOI

10.1175/jcli-d-23-0286.1

Copyright Information

Peer reviewed

The Influence of ENSO Diversity on Future Atlantic Tropical Cyclone Activity

Teryn J. Mueller,[a] Christina M. Patricola,[a,b] and Emily Bercos-Hickey[b]

[a] *Department of Geological and Atmospheric Sciences, Iowa State University, Ames, Iowa*
[b] *Climate and Ecosystem Sciences Division, Lawrence Berkeley National Laboratory, Berkeley, California*

ABSTRACT: El Niño–Southern Oscillation (ENSO) influences seasonal Atlantic tropical cyclone (TC) activity by impacting environmental conditions important for TC genesis. However, the influence of future climate change on the teleconnection between ENSO and Atlantic TCs is uncertain, as climate change is expected to impact both ENSO and the mean climate state. We used the Weather Research and Forecasting Model on a tropical channel domain to simulate 5-member ensembles of Atlantic TC seasons in historical and future climates under different ENSO conditions. Experiments were forced with idealized sea surface temperature configurations based on the Community Earth System Model (CESM) Large Ensemble representing: a monthly varying climatology, eastern Pacific El Niño, central Pacific El Niño, and La Niña. The historical simulations produced fewer Atlantic TCs during eastern Pacific El Niño compared to central Pacific El Niño, consistent with observations and other modeling studies. For each ENSO state, the future simulations produced a similar teleconnection with Atlantic TCs as in the historical simulations. Specifically, La Niña continues to enhance Atlantic TC activity, and El Niño continues to suppress Atlantic TCs, with greater suppression during eastern Pacific El Niño compared to central Pacific El Niño. In addition, we found a decrease in the Atlantic TC frequency in the future relative to historical regardless of ENSO state, which was associated with a future increase in northern tropical Atlantic vertical wind shear and a future decrease in the zonal tropical Pacific sea surface temperature (SST) gradient, corresponding to a more El Niño–like mean climate state. Our results indicate that ENSO will remain useful for seasonal Atlantic TC prediction in the future.

KEYWORDS: Teleconnections; ENSO; Hurricanes/typhoons; Tropical cyclones; Climate change; Regional models

1. Introduction

Tropical cyclones (TCs) are both damaging and deadly, with $1.387 trillion in damages and 6897 deaths in the United States between 1980 and 2023 (Smith 2022; NOAA NCEI 2024). Due to the high economic costs and safety threats posed by TCs, there is an urgent need to improve future projections of TC activity. To better project future changes in TC activity, it can be informative to consider patterns of climate variability that create seasonal anomalies in the necessary ingredients for TC genesis, including warm sea surface temperatures (SSTs), a moist midtroposphere, atmospheric instability, and weak vertical wind shear. One major influence on seasonal TC activity in several basins is El Niño–Southern Oscillation (ENSO) (e.g., Lin et al. 2020)—the leading mode of tropical climate variability.

The positive phase of ENSO, or El Niño, is characterized by warm SST anomalies (SSTAs) in the central-eastern equatorial tropical Pacific, whereas the negative phase, La Niña, is characterized by cool SSTAs in the same region. Along with these SSTAs, ENSO also causes fluctuations in the Walker circulation (Bjerknes 1966), the large-scale zonal and vertical atmospheric circulation over the tropics, by shifting the location of deep convection in the tropical Pacific and altering tropical upper-tropospheric and lower-tropospheric zonal winds.

ENSO's modulation of the Walker circulation—through shifting the location of tropical Pacific deep convection and changing lower- and upper-level winds—impacts vertical wind shear, relative humidity, and instability over the Atlantic TC genesis region. Many studies have found that compared to La Niña and ENSO neutral conditions, El Niño events drive a decrease in the frequency and intensity of Atlantic TCs by increasing Atlantic vertical wind shear (e.g., Gray 1984; Goldenberg and Shapiro 1996; Bove et al. 1998; Landsea et al. 1999; Pielke and Landsea 1999; Smith et al. 2007; Klotzbach et al. 2017; Lin et al. 2020). This relationship between El Niño and Atlantic vertical wind shear exists due to warm SSTAs in the equatorial eastern-central Pacific, which shift tropical Pacific deep convection eastward, causing upper-level westerly wind anomalies and increased vertical wind shear over the Atlantic TC main development region (e.g., Horel and Wallace 1981; Hoerling and Kumar 2002). Likewise, La Niña enhances Atlantic TC development by weakening vertical wind shear in the Atlantic. In addition, instability and relative humidity, two other factors important for Atlantic TCs, decrease during El Niño (Camargo et al. 2007a) due to anomalous upper-tropospheric warming (Chiang and Sobel 2002; Tang and Neelin 2004), which also stems from a shift in the Walker circulation.

To fully explain ENSO's influence on Atlantic TCs, we must consider variations in the spatial patterns of SSTAs during El Niño events, often referred to as ENSO diversity (e.g., Capotondi et al. 2015a; Timmermann et al. 2018; Capotondi et al. 2020).

These variations in El Niño events are often categorized into two groups, known as eastern Pacific El Niño and central Pacific El Niño (or El Niño Modoki) (Ashok et al. 2007; Kao and Yu 2009). Eastern Pacific (EP) El Niño is characterized by maximum SST warming in the eastern tropical Pacific, whereas central Pacific (CP) El Niño is characterized by maximum SST warming in the central tropical Pacific, with SSTAs tending to be stronger during EP El Niño compared to CP El Niño. A third "mixed El Niño" category was introduced to account for El Niño events that share attributes from both categories (Kug et al. 2009; Ashok et al. 2012), as CP and EP El Niño do not represent the full spectrum of spatial patterns of SSTAs. As described above, tropical Pacific deep convection shifts eastward and strongly impacts upper-tropospheric winds during El Niño; the nature of this response depends on both the magnitude and location of the SSTAs and, therefore, depends on the type of El Niño event (Patricola et al. 2016). La Niña, on the other hand, has a relatively smaller longitudinal shift in deep convection (Kug et al. 2009; Kug and Ham 2011; Ren and Jin 2011). Although the differences in spatial patterns of SSTAs during El Niño events tend to be more pronounced during ENSO's boreal winter peak, compared to the hurricane season's boreal autumn peak, ENSO diversity is nonetheless important in modulating the zonal shifts in tropical Pacific deep convection that influence Atlantic hurricane seasons (Patricola et al. 2016).

ENSO diversity can substantially modulate the teleconnection between ENSO and Atlantic TCs in the present climate, as found in climate simulations forced with observed SST patterns characteristic of the different El Niño types (Patricola et al. 2016). The climate model simulations demonstrated that CP El Niño suppressed Atlantic TCs, but was less effective at doing so than EP El Niño for magnitudes of SST warming corresponding to strong observed events (i.e., stronger warming for EP El Niño compared to CP El Niño). The response in Atlantic TCs was driven primarily by changes in vertical wind shear, with secondary contributions from relative humidity. Note that this is similar to the reanalysis-based findings of Camargo et al. (2007b) in that wind shear and relative humidity are important contributors to ENSO's influence on Atlantic TCs. Camargo et al. (2007b) found that relative humidity was the most important factor, but we note that older reanalysis data such as the NCEP/NCAR I (Kalnay et al. 1996) used in their study have large uncertainty in relative humidity estimates. The strength of the wind shear and humidity responses were related to the zonal shifts in tropical Pacific deep convection and the Walker circulation, which depended on the magnitude and location of the SSTA forcings (Patricola et al. 2016).

A major gap in our understanding of the ENSO–TC teleconnection is how ENSO's influence on seasonal Atlantic TC activity in the historical climate may be altered by future greenhouse gas emissions (Lin et al. 2020), potentially through changes in ENSO (including frequency, intensity, and diversity), as well as through changes in the tropical Pacific SST climatology associated with mean climate change, including possible changes in tropical Pacific zonal SST gradients. Projecting future changes in ENSO is a challenge, as there is no agreement on future changes in the ENSO frequency, amplitude, subsurface ocean temperatures, and ENSO diversity (e.g., Ashok et al. 2007; Yeh et al.

2009; Collins et al. 2010; Lee and McPhaden 2010; Kug et al. 2012; Kim and Yu 2012; Stevenson 2012; Yeh et al. 2014; Zheng et al. 2016).

One major reason for this lack of agreement in changes in ENSO involves uncertainty in the future of the tropical Pacific zonal SST gradient (e.g., Seager et al. 2019; Lee et al. 2022). Part of this uncertainty stems from coupled global climate models (GCMs) suffering from substantial biases in climatological SSTs in the eastern tropical Pacific (Richter 2015; Zuidema et al. 2016). The occurrence of these biases in the ENSO region can directly impact simulated ENSO variability (e.g., Capotondi et al. 2015b) and can influence future projections of ENSO (Tang et al. 2021). Along with these GCM biases, state-of-the-art climate models, such as those participating in phase 5 of the Coupled Model Intercomparison Project (CMIP5) and phase 6 of CMIP (CMIP6), produce a general agreement that the mean tropical Pacific zonal SST gradient will weaken (i.e., become more El Niño–like) in the future (An et al. 2008; Cai et al. 2015; Fredriksen et al. 2020; Erickson and Patricola 2023), even though recent observations have suggested that the opposite has been occurring (Seager et al. 2019; Zhao and Allen 2019). This discrepancy between the recently observed La Niña–like trends and the future projections of El Niño–like trends has caused uncertainty in future ENSO projections (e.g., Seager et al. 2019; Tang et al. 2021), as the reliability of the GCMs has been questioned due to their large biases in the eastern Pacific cold tongue. Given the complexity of simulating ENSO and the uncertainty of how model biases may impact future ENSO projections, substantial uncertainty exists regarding how ENSO may change in the future.

Along with the uncertainty in future changes in ENSO, there is also uncertainty in how greenhouse gas (GHG) emissions have influenced North Atlantic TC frequency (e.g., Knutson et al. 2019) and will influence it in the future (e.g., Pielke et al. 2005; Bengtsson et al. 2007; Gualdi et al. 2007; Garner et al. 2009; Knutson et al. 2010, 2020). Notably, understanding the controls on global TC frequency remains an elusive problem for which there is no theory (Sobel et al. 2021). As for TC intensity, there is better agreement that TCs will become stronger in the future (e.g., Bengtsson et al. 2007; Elsner et al. 2008; Knutson et al. 2010; Yu et al. 2010; Zhao and Held 2010; Walsh et al. 2016; Knutson et al. 2020).

An important key to projecting future changes in Atlantic TC activity lies in understanding how the current ENSO–Atlantic TC teleconnection, as well as ENSO itself, may change with GHG emissions. This multifaceted problem is split into three questions: 1) How will GHG emissions impact ENSO? 2) How will GHG emissions impact climatological Atlantic TC frequency and intensity? 3) How will the existing teleconnection between ENSO and Atlantic TCs change in the future?

The primary focus of this paper is to understand how the current teleconnection between ENSO and Atlantic TCs could change in the future. Given that environmental conditions important for TC genesis (e.g., vertical wind shear) may be altered by future changes in ENSO and the mean climate, it is possible that the ENSO–TC teleconnection could change with a changing climate; this is especially the case given the importance of thresholds in the response of TCs to vertical wind shear (Tao and Zhang 2014). We will also work toward addressing how ENSO

may change in the future and how Atlantic TC activity may change in association with mean climate change irrespective of ENSO. Here, we performed simulations using the Weather Research and Forecasting (WRF) Model to simulate how seasonal Atlantic TC activity responds to different phases of ENSO in historical and future climates. We used the Community Earth System Model, version 1 (CESM1), Large Ensemble (LENS; Kay et al. 2015) to create idealized SST patterns representing the different phases of ENSO in both climate states. We used SST data from a large 35-member ensemble, rather than multimodel ensembles such as CMIP6 which tend to have relatively few ensemble members from each model, in order to have sufficient sample sizes of ENSO events. Large ensembles also are best suited to quantify future changes in ENSO, as internal variability is large compared to future anthropogenic changes in ENSO (Maher et al. 2018; Zheng et al. 2018; Lee et al. 2021). This paper first investigates future ENSO projections in CESM LENS and then uses CESM LENS to create SST forcings representative of various ENSO patterns. We then ran WRF experiments and analyzed Atlantic TC frequency and intensity during ENSO events in the historical climate. We evaluated the influence of future changes in the mean climate state on Atlantic TCs before finally investigating possible changes in the teleconnection between ENSO and Atlantic TCs by comparing historical and future simulations forced by idealized ENSO scenarios. Developing an understanding of the influence of climate change on the ENSO–Atlantic TC relationship addresses a major knowledge gap identified by the scientific community (Lin et al. 2020).

2. Data

a. Observational datasets

Observed SST is based on the Extended Reconstructed Sea Surface Temperature, version 5 (ERSSTv5), which has global, monthly data from 1854 to the present at a resolution of 2.0° latitude × 2.0° longitude (Huang et al. 2017). We used ERSSTv5 to identify observed ENSO events and to serve as the basis for the model bias correction.

The initial, surface boundary, and lateral boundary conditions for the WRF historical climate simulations were based on the 6-hourly, 2.5° latitude × 2.5° longitude resolution National Centers for Environmental Prediction (NCEP-II) reanalysis (Kanamitsu et al. 2002).

Observational TC data were obtained from the Atlantic hurricane database (HURDAT2; Landsea and Franklin 2013) as archived in the International Best Track Archive for Climate Stewardship (IBTrACS; Knapp et al. 2010). HURDAT2 extends from 1851 to the present and includes 6-hourly location and intensity information. HURDAT2 has a potential low bias in the presatellite era (before 1966 in the North Atlantic) due to observational limitations, which must be considered when investigating TC trends (Vecchi and Knutson 2008, 2011; Vecchi et al. 2021).

b. CESM large ensemble data

SST forcings and future climate change perturbations for the WRF simulations were constructed from the CESM LENS (Kay et al. 2015). CESM LENS is a set of coupled atmosphere–ocean climate model simulations performed with the nominal 1° latitude/longitude version of CESM, version 1. CESM LENS has 40 ensemble members and covers the years 1920–2100, with the representative concentration pathway 8.5 (RCP8.5) used for future climate simulations from 2006 to 2100. We used 35 ensemble members, which included the data accessible at the time of this study.

3. Methods

a. ENSO index

To identify ENSO events, we used the ENSO longitude index (ELI), which can capture ENSO diversity by estimating zonal variations in tropical Pacific deep convection associated with ENSO (Williams and Patricola 2018). The ELI is calculated for each month by 1) calculating the tropical-average SST (i.e., convective threshold), 2) identifying which points in the tropical Pacific meet or exceed the tropical-average SST, and 3) calculating the average longitude for the points that satisfy the second condition (Williams and Patricola 2018). This index was chosen over other ENSO metrics, such as the Niño 3.4 index, as the ELI is unique in capturing ENSO diversity in one index, whereas Niño-3.4 is unable to capture ENSO diversity due to its construction (SSTA over a fixed region). In addition, the ELI has demonstrated value in operational seasonal Atlantic TC prediction (Klotzbach et al. 2022). Since the ELI represents the longitude of tropical Pacific deep convection, it captures the most important difference between each ENSO state that causes the teleconnection with Atlantic TC frequency. Although the ELI does not directly measure SSTA strength, the ELI and the Niño-3.4 index are strongly correlated during the August–October Atlantic hurricane season peak ($R = 0.91$ over the period 1950–2022). In addition, the ELI is able to distinguish between EP and CP El Niño events during boreal summer, as shown in Fig. 1b from Williams and Patricola (2018). An important difference between the ELI and the Niño-3.4 index is that the ELI more clearly identifies extreme El Niño events during boreal winter (Fig. 1a from Williams and Patricola 2018), where an extreme El Niño event is one characterized by both strong SSTAs and a strong eastward shift in tropical Pacific deep convection. In addition, the Niño-3.4 index quantifies SSTAs but is not designed to capture zonal shifts in deep convection.

b. Regional climate model simulations

We performed regional climate model simulations using the WRF Model, version 4.3.3 (Skamarock et al. 2019). The WRF simulations used an atmosphere-only model in order to prescribe ENSO conditions and to mitigate basin-scale SST biases that can cause errors in simulations of TCs (Hsu et al. 2019). SSTs were prescribed from CESM LENS data, as explained in section 3b(2). The WRF experiments use a 27-km resolution tropical channel model (TCM) domain that covers 30°S–50°N around the globe (Fig. 1), with 48 vertical layers from the surface to 50 hPa and a 60-s time step (Patricola et al. 2016; Fu et al. 2019). This resolution is high enough to
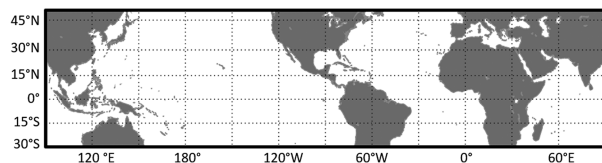
FIG. 1. Domain used in the WRF simulations (30°S–50°N, 180°–180°).

represent TCs and allows a large domain suitable for capturing the influence of ENSO on the Atlantic. We note that at 27 km, the model struggles to simulate intense TCs (category 3 and stronger), as expected given the resolution (Davis 2018).

The initial, lateral boundary, and land surface boundary conditions were based on the 6-hourly NCEP-II reanalysis data from 1989, a year characterized by a near-neutral phase of the Atlantic multidecadal oscillation (AMO), to minimize potential influences of the midlatitude lateral boundary conditions (LBCs) on the simulation (Patricola et al. 2016). This was done because the AMO has a substantial influence on Atlantic TC activity (Goldenberg et al. 2001; Bell and Chelliah 2006). Previous research has found little sensitivity to the year selected for LBCs for TCM simulations involving TC applications (Patricola et al. 2016). The simulation length was from 1 May to 1 December, which was chosen to include the Atlantic hurricane season (1 June–30 November), along with an additional month for model spinup. Each of the five ensemble members per experiment was made under the same GHG concentrations and SST forcings, with slightly different initial conditions created by starting the runs on different days (1–5 May). The experiments were limited to five ensemble members due to computational expenses; however, this ensemble size is suitable for such applications (Lee et al. 2021) and was sufficient to reveal climate change responses. The model parameterizations are consistent with the TCM configuration from Patricola et al. (2014) and were chosen for their ability to reasonably reproduce TC frequency at 27-km resolution.

1) CLIMATE SCENARIOS

We performed experiments representing two climate states, namely, a historical (1980–2000) and a future (2080–2100) climate (Table 1), with each climate state including four prescribed ENSO conditions discussed in the next section. For the historical climate, LBCs were based on 6-hourly NCEP-II reanalysis, whereas SSTs were prescribed using ENSO composites developed from the CESM LENS over 1980–2000 [see section 3b(2)]. For SSTs, 21 years were sufficient to represent 95% of the internal variability of ENSO (Maher et al. 2018), considering the use of 35 ensemble members. The GHG concentrations for the historical climate (Table 2) were prescribed according to the World Data Center for Greenhouse Gases (Tsutsumi et al. 2009) and the Carbon Dioxide Information Analysis Center (Bullister and Warner 2015).

The future climate simulations were created using the pseudo–global warming approach (Schär et al. 1996) for the LBCs and initial conditions, with prescribed bias-corrected SSTs. Specifically, the 6-h NCEP-II reanalysis data from 1989 were used for the initial, lateral, and surface boundary conditions, but with additional climate change differences, or deltas, prescribed to the temperature, pressure, and humidity-related variables. The deltas were created by calculating the difference between the future climate (2080–2100) and the historical climate (1980–2000) CESM LENS data, and accounted for spatial (horizontal and vertical) and seasonal variations in the future change. SSTs were prescribed from the CESM LENS, with forcings created using the years 2080–2100. The pseudo–global warming approach for the LBCs and initial conditions creates a future climate that has a realistic estimation of the mean state, while using SSTs from CESM LENS allows us to account for potential changes in ENSO's spatial patterns and magnitude. The RCP8.5 emissions scenario was used to represent GHG concentrations at the end of the twenty-first century (Table 2; Riahi et al. 2011). RCP8.5 is the high-end estimate for global mean temperature increase by the end of the twenty-first century and represents what are currently considered to be the potential maximum impacts of climate change in the next century.

2) SST FORCINGS

We performed WRF experiments using SST forcings representing four different ENSO conditions, including monthly varying climatological SST (neutral ENSO), central Pacific El Niño, eastern Pacific El Niño, and La Niña, in each of the historical and the future climates (Table 1). These SST configurations were created with the CESM LENS data.

TABLE 1. Summary of WRF experiments performed, including climate state (historical, 1980–2000 and future, 2080–2100), SST forcing, ELI values used to categorize the ENSO SST forcings, and number of years in each SST composite (out of a possible 735 total years).

Climate state	SST forcing	ELI values	Number of years in SST composite
Historical	Climatological	—	735
Historical	Central Pacific El Niño	175°E–180°	36
Historical	Eastern Pacific El Niño	East of 190°E	6
Historical	La Niña	West of 160°E	66
Future	Climatological	—	735
Future	Central Pacific El Niño	175°E–180°	56
Future	Eastern Pacific El Niño	East of 190°E	17
Future	La Niña	West of 160°E	181

TABLE 2. GHG concentrations prescribed in the historical and future climate WRF simulations, with units in parts per million (ppm), parts per billion (ppb), or parts per trillion (ppt).

GHG	Historical	Future
Carbon dioxide (CO_2)	354 ppm	845 ppm
Methane (CH_4)	1723 ppb	3640 ppb
Trichlorofluoromethane (CFC-11)	265 ppt	357 ppt
Dichlorodifluoromethane (CFC-12)	497 ppt	196 ppt
Nitrous oxide (N_2O)	308 ppb	421 ppb
Chlorodifluoromethane (CFC-22)	169 ppt	143 ppt
Carbon tetrachloride (CCl_4)	104 ppt	93 ppt

The climatological monthly SSTs were calculated by first creating the monthly averages for each climate state (1980–2000 and 2080–2100) using all 35 ensemble members and then subtracting the model biases from them. The model bias was calculated by taking the CESM climatological monthly average of 1980–2000 and subtracting the ERSSTv5 observed monthly average SSTs of the same years. We used the SST bias of the historical period for the future period, which assumes that the bias is unchanged in the future. We note that this procedure corrects only for mean-state SST biases, which is relatively straightforward, and does not correct for any biases in ENSO characteristics and variability.

The SST patterns for each of the three ENSO states in both the historical (Figs. 2b,e,h) and future climates (Figs. 2c,f,i) were calculated using composites of SSTs based on the ELI. In particular, ENSO events were identified based on ELI averaged over August, September, and October (ASO) for each simulated CESM LENS year, to represent the peak hurricane season when the teleconnection between ENSO and Atlantic

TCs is strongest. We note that while the ASO average was used to identify ENSO events, the SST forcings use the monthly SST. This choice does not change the sample size of events. We used the 10th (west of 160°E) and 90th (east of 175°E) percentile ELI values from ERSSTv5 observations over 1854–2020 to define the ENSO state (La Niña and El Niño, respectively). The range of ASO ELI values in CESM LENS was roughly 175°–200°E for El Niño and 155°–160°E for La Niña. For our final SST configurations prescribed to WRF, we used the ASO ELI bin that was west of 160°E to represent La Niña, the ASO ELI bin 175°E–180° to represent central Pacific El Niño, and the ASO ELI east of 190°E to represent eastern Pacific El Niño. The extremes of the ELI were chosen to represent the range of ENSO diversity. We note that the ELI values typical of El Niño and La Niña events depend on the season; therefore, different values are used to identify ENSO events in ASO compared to December–February. We chose to define the eastern Pacific and central Pacific El Niño events with a gap in the ELI of 10° of longitude in between, to clearly capture the two distinct patterns. The events with the ELI in between tended to correspond to mixed El Niño events with warm SSTAs in both the eastern and central Pacific. This mixed El Niño pattern was not used as forcing for WRF simulations in this study due to the primary focus on the eastern Pacific El Niño and central Pacific El Niño events, as well as computational limitations. We suspect that the mixed El Niño pattern would have produced results in between those from the eastern Pacific and central Pacific El Niño events.

Each of the events from all of the ensemble members categorized in each ELI bin was averaged to create a monthly SST composite representing each ENSO state. We note that
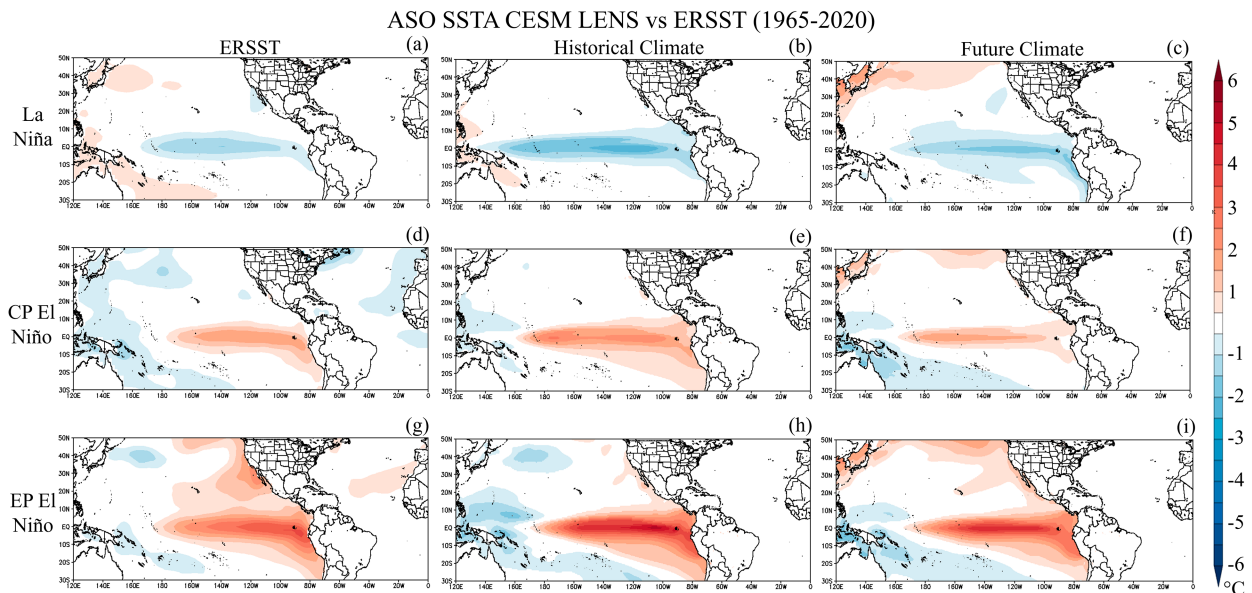

FIG. 2. ASO SSTAs (°C) from composites of (top) La Niña, (middle) CP El Niño, and (bottom) EP El Niño events from the ERSSTv5 observations over (left) 1965–2020, (center) the CESM LENS historical simulation, and the (right) CESM LENS future simulation. The observed composites included 1973, 1975, 1988, 1998, 1999, 2010, 2016, and 2020 for La Niña, 1965, 1972, and 1982 for CP El Niño, and 1997 and 2015 for EP El Niño.

the ENSO SST forcings were applied only over the Pacific basin; all other basins were prescribed the monthly SST corresponding to the climatology for the given climate state (i.e., historical or future). This was done to control the SSTs such that ENSO was the only major SST pattern changing between each experiment. The SSTs were corrected for the monthly model bias.

The SSTA composites for ENSO events from the historical CESM LENS simulations (Figs. 2b,e,h) reasonably capture the patterns expected based on observations (Figs. 2a,d,g). There are some relatively minor differences between the observed and CEMS LENS historical SSTAs, with stronger SST cooling (warming) during historical La Niña (EP and CP El Niño) and maximum EP El Niño SSTAs shifted slightly from the east Pacific toward the central Pacific in CESM compared to observations. Furthermore, the SSTA composites for ENSO events in the future CESM LENS simulations retain the signatures of the corresponding historical events. We emphasize that the SSTAs alone do not fully represent the strength of ENSO events, which also depend on changes in the mean-state SST.

3) TC TRACKING

We tracked simulated Atlantic TCs every 6 h using the algorithm of Walsh (1997), which included criteria that the system must have a warm core, be a closed-off low, have a 850-hPa mean wind speed greater than the 300-hPa mean wind speed, have a minimum 10-m wind speed of 17.5 m s^{-1}, and an additional requirement that TCs last longer than 2 days to avoid minor disturbances influencing results. These requirements detect systems that meet the standard to be considered at least a tropical storm. Accumulated cyclone energy (ACE; Bell et al. 2000) was also calculated for each TC and then summed for each season by adding all of the squared 6-hourly maximum 10-m wind speeds together for each TC over the whole season and dividing by 10 000. The ACE (10^4 kt^2; 1 kt $\approx$ 0.51 m s^{-1}) was calculated because it is a more comprehensive metric for TC activity that considers the TC number, intensity, and duration.

4. Results

a. ENSO and mean-state SST in the CESM LENS

We first compared ENSO during ASO in the historical CESM LENS with observations to determine any model biases. The LENS historical simulations reproduced the frequency of El Niño events reasonably well while doubling the frequency of La Niña events compared to observations, which is apparent in the ELI distribution and histograms (Figs. 3a,c). In addition, although the LENS reproduced the frequency of observed El Niño events well, the LENS simulated El Niño events with stronger magnitudes than observed. We also compared composites of SSTAs for El Niño and La Niña events from the CESM LENS historical simulations (Figs. 2b,e,h) and observations (Figs. 2a,d,g) and found that the SSTAs are reasonably similar between the two, albeit with stronger SSTAs in LENS than in observations.
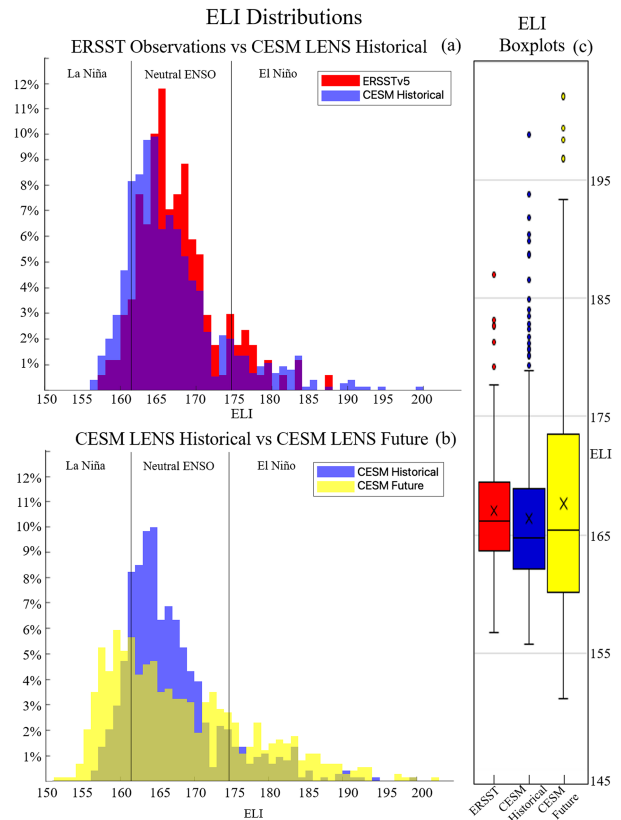

FIG. 3. Histograms showing ASO averaged ELI (°E) from (a) ERSSTv5 observations (red) over the years 1854–2022 compared to CESM LENS over the years 1980–2000 and from 35 ensemble members, and (b) CESM LENS over the years 1980–2000 compared to CESM LENS over the years 2080–2100 (yellow). The two lines represent the ELI values used to characterize either El Niño or La Niña. (c) The boxplot compares the ASO ELI (°E) values from ERSSTv5 observations and the CESM LENS historical and future simulations, with the x mark representing the average.

Having evaluated how well the CESM LENS historical simulation represents observed ENSO frequency and magnitude, we then investigated how the CESM LENS projects ENSO to change in the future. We found that the CESM LENS projects a substantial increase in the number of extreme ENSO events during ASO, similar to the projected change during boreal winter (Williams and Patricola 2018), along with a change in the mean state toward more El Niño–like conditions (Figs. 3b,c). This shift to more El Niño–like conditions is consistent with the future SST warming pattern in CESM LENS, with greater warming over the eastern Pacific cold tongue than in the surrounding areas (Fig. 4c).

b. Influence of ENSO on Atlantic TCs in the historical climate

We compared TC activity in the WRF historical simulations with observations to gauge how well the model represents TC activity and its response to ENSO. Overall, the WRF historical climatology simulation produced more Atlantic TCs than
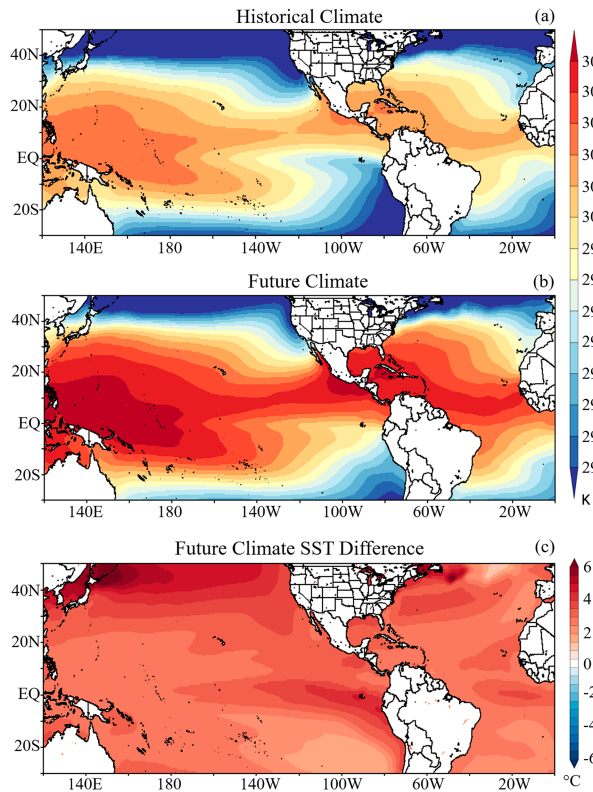
FIG. 4. Climatological ASO SSTs (K) from the (a) historical CESM LENS simulation over 1980–2000, (b) future CESM LENS simulation over 2080–2100, and (c) the difference between the future minus the historical simulations. The SSTs represent the mean state prescribed for the historical and future WRF simulations.

observations, with 59% more Atlantic TCs and 18% more ACE per year than the observed climatology (Table 3). The bias in the TC count was greater than the bias in ACE, which is likely associated with the inability of the model to represent intense TCs due to its resolution. We note that despite the lack of intense TCs (category 4 and 5 hurricanes) in the model, the model is able to simulate changes in TC intensity in response to ENSO and climate change. For this reason, and because ACE is a commonly used metric for TC activity, we included ACE in the analysis despite the limitation that the model fails to simulate the most intense TCs.

The TC track density from the 5-member ensemble of the historical simulations clearly shows a decrease in the Atlantic TC frequency in both historical El Niño experiments (Figs. 5c,e) compared to the historical climatology simulation (Fig. 5a), whereas La Niña produced a moderate increase in the TC frequency (Fig. 5g). The Atlantic TC response simulated by WRF is consistent with the observed TC response during El Niño and La Niña (Table 3), although internal atmospheric variability was not well accounted for due to the small sample sizes for observed El Niño events. Relatively few observed El Niño events, along with the use of different EP El Niño ELI bins between the observations and the simulations, could explain the differences between the observed and simulated influence of CP and EP El Niño on Atlantic TC activity. SST conditions in the Atlantic also impact observed TC activity, as the Atlantic Meridional Mode (AMM) was positive for both observed EP El Niño years, which would cause less suppression of Atlantic TCs than the EP El Niño would cause with a neutral AMM (Patricola et al. 2014; Klotzbach 2011).

We quantified the Atlantic TC activity response to ENSO using the number of TCs per year and ACE. The 5-member ensemble of historical climatology simulations produced an average of 20 TCs per year and an average seasonal ACE of 120.7 (Table 3). In response to the ENSO SST forcings in the historical climate, the WRF simulations produced a 55% decrease in TCs per year and a 58% decrease in the ACE per year during eastern Pacific El Niño relative to the climatology simulation (Table 3). This simulated suppression of TCs was greater than observed, likely due to the differences in ELI used to define El Niño and influences outside of the Pacific, such as the AMM, on the observed findings. The central Pacific El Niño simulations produced a 39% decrease in Atlantic TCs per year and a 44% decrease in the ACE per year compared to the climatological simulations (Table 3), which is relatively similar to observations. Atlantic TC suppression was less effective in the CP El Niño experiment compared to the EP El Niño experiment, consistent with Patricola et al. (2016). This indicates that Atlantic TC suppression is greater the further east that tropical Pacific deep convection is located. This response is not well characterized in the limited historical observations of CP and EP El Niño but is apparent when comparing El Niño to the climatology and La Niña simulations. The historical La Niña simulation produced a moderate 8% increase in Atlantic TCs per year and an 11% increase in the ACE per year (Table 3) compared to the climatology simulation. The

TABLE 3. Average values and percent change relative to climatology (in parentheses) in the seasonal Atlantic number of TCs and ACE (10^4 kt^2) from (left) IBTrACS observations and (right) the historical WRF experiments. Each WRF experiment had a different SST forcing representing either La Niña, CP El Niño, or EP El Niño. The ELI bin and sample or ensemble size used to configure the SSTAs are shown. ENSO events during the years 1965–2020 were identified based on the ASO ELI from ERSSTv5 observations.

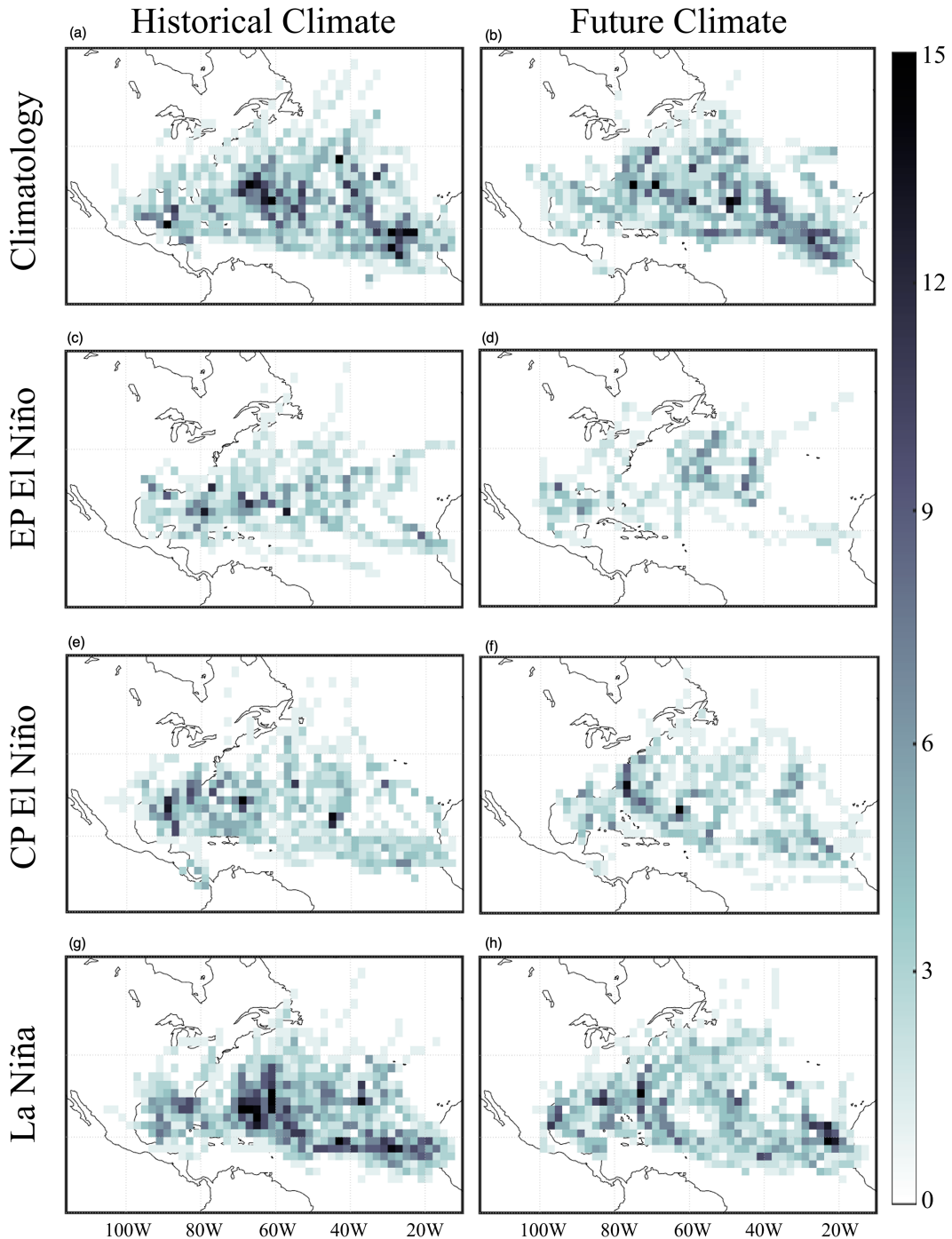| ENSO state	Observations (1965–2020)				WRF historical simulations			
	Climo	EP El Niño	CP El Niño	La Niña	Climo	EP El Niño	CP El Niño	La Niña
Sample or ensemble size	55	2	3	8	5	5	5	5
ELI bin	—	East of 180°	175°E–180°	West of 160°E	—	East of 190°E	175°E–180°	West of 160°E
Number of TCs	12.6	9.5 (−24%)	7.7 (−40%)	14.9 (19%)	20	9 (−55%)	12.2 (−39%)	21.6 (8%)
ACE	102.6	51.81 (−50%)	50.5 (−51%)	134 (31%)	120.7	50.5 (−58%)	67.1 (−44%)	134.2 (11%)

FIG. 5. Atlantic TC track density (TCs per 6 h over the 5-member ensemble) over 1 Jun–30 Nov from the 5-member ensemble of the WRF simulations under prescribed SST forcings representing (a),(b) climatology, (c),(d) EP El Niño, (e),(f) CP El Niño, and (g),(h) La Niña for the historical and future climates, respectively.

difference in TC activity between La Niña and the climatology was weaker in the WRF simulations compared to observations, although both increased TCs and seasonal ACE during La Niña. The increase in the ensemble-mean number of TCs in the La Niña historical simulation was less than one standard deviation above the ensemble-mean number of TCs in the control historical simulation.

To understand the physical mechanisms driving the Atlantic TC response to ENSO, we investigated vertical wind shear (VWS) between 850 and 200 hPa and 700-hPa relative humidity (RH) in
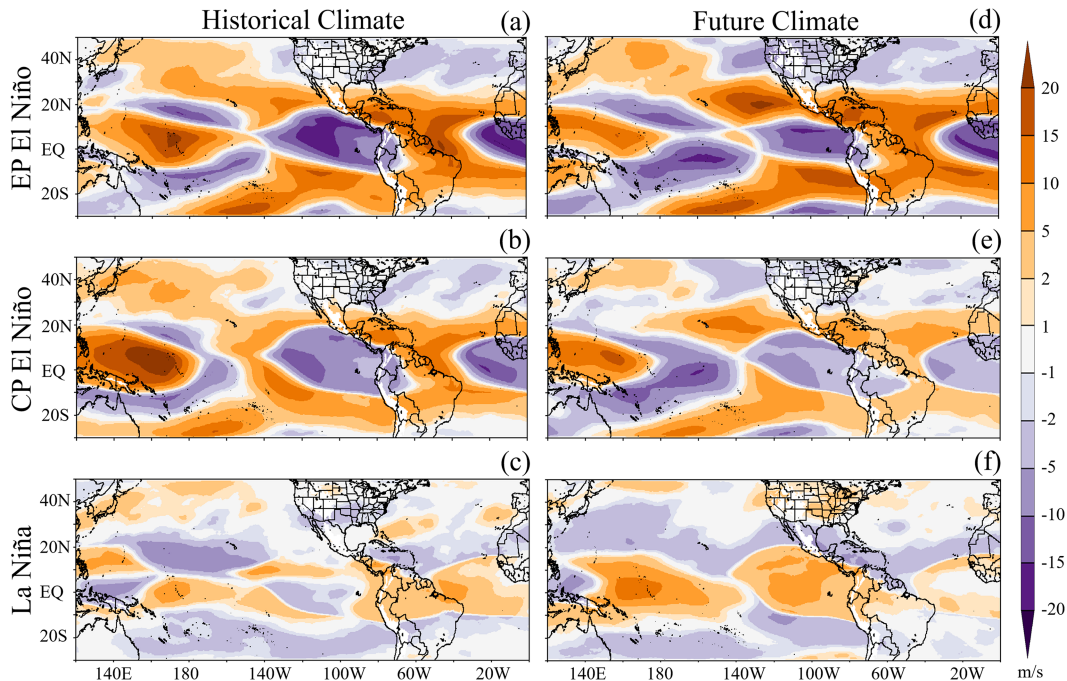
FIG. 6. Response in the ASO zonal 850–200-hPa vertical wind shear (m s^{-1}) from the historical climate (a) EP El Niño, (b) CP El Niño, and (c) La Niña simulations minus the historical climatology simulation and the future climate (d) EP El Niño, (e) CP El Niño, and (f) La Niña simulations minus the future climatology simulation, based on the 5-member ensemble of the WRF simulations.

the historical simulations. We focused on physical variables impacted by ENSO instead of using the genesis potential index (GPI), which considers the aforementioned large-scale variables, together with low-level vorticity and potential intensity, together. We chose this approach because metrics like GPI can poorly explain future changes in TCs (Camargo 2013), likely because the GPI is an empirical index developed using historical climate data. There is an increase in VWS over most of the Atlantic TC genesis region for both El Niño types and a decrease in VWS for La Niña in the historical climate (Figs. 6a–c). EP El Niño produced VWS enhancements of up to 10 m s^{-1} over the Atlantic TC genesis region (Fig. 6a). This large anomaly caused the average VWS over a substantial portion of the Atlantic TC genesis region to change from a range of 0–7.5 m s^{-1} to a range of 10–20 m s^{-1} (not shown). This is important because VWS exceeding values of 10–12 m s^{-1} is typically unfavorable for TCs (Zhang and Tao 2013; Tao and Zhang 2014, 2015; Rios-Berrios and Torn 2017). CP El Niño enhanced VWS (Fig. 6b), but not as strongly as EP El Niño, resulting in most of the Atlantic TC genesis region increasing from an ASO average VWS of 0–7.5 to 5–17.5 m s^{-1} (not shown). The historical La Niña simulations produced a slight reduction in VWS (2–5 m s^{-1}) over much of the Atlantic TC genesis region (Fig. 6c), consistent with the slight increase in Atlantic TC activity. The simulated VWS response to ENSO is closely related to the 200-hPa zonal wind response (not shown), which is driven by the location of tropical Pacific deep convection. Therefore, the longitude of maximum tropical Pacific deep convection indicates the main physical

mechanisms by which the ENSO teleconnection influences Atlantic TC activity.

Midtropospheric RH decreased during El Niño and increased during La Niña over much of the northern tropical Atlantic in the historical simulations (Figs. 7a–c), although compared to VWS, RH is less correlated with the Atlantic TC frequency response. In both El Niño simulations, RH slightly decreased over most of the Atlantic TC genesis region (Figs. 7a,b), which, along with the VWS response, helped explain the suppression of Atlantic TCs in both El Niño experiments. However, CP El Niño produced a stronger RH response than EP El Niño. This shows that the 200-hPa zonal wind and VWS responses are better indicators of the Atlantic TC suppression; in particular, the EP El Niño simulation produced roughly 25% fewer TCs than CP El Niño, which is consistent with the larger increase in VWS but inconsistent with the smaller decrease in RH during EP El Niño compared to CP El Niño. This leads us to conclude that VWS is generally the primary explanation for the Atlantic TC response to ENSO, whereas RH is a secondary influence.

Overall, the results from the historical WRF experiments match the current understanding of ENSO's influence on Atlantic TCs. Our findings agree with the established influence El Niño has on Atlantic TCs, including the overall Atlantic TC reduction during El Niño (e.g., Gray 1984 and others), the differences in the TC response between CP and EP El Niño (Patricola et al. 2016), and the slight increase in Atlantic TCs during La Niña. Finally, Atlantic VWS responses driven by the zonal shift in the tropical Pacific deep convection and associated 200-hPa zonal wind response are consistent with previous research and
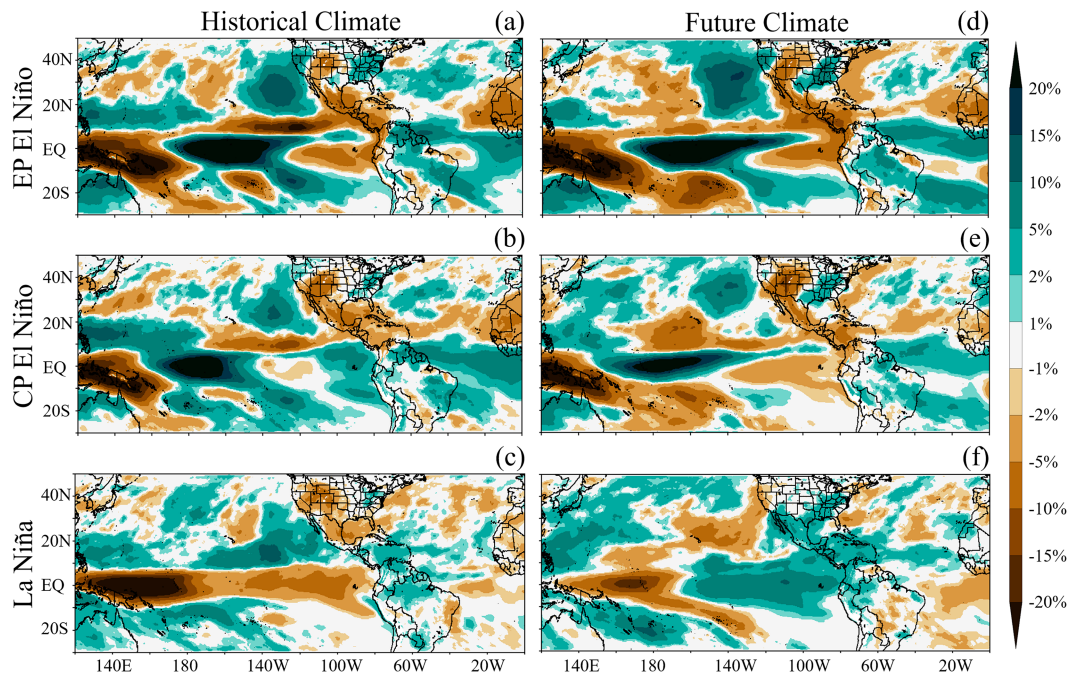
FIG. 7. Response in the ASO 700-hPa relative humidity (%) from the historical climate (a) EP El Niño, (b) CP El Niño, and (c) La Niña simulations minus the historical climatology simulation and the future climate (d) EP El Niño, (e) CP El Niño, and (f) La Niña simulations minus the future climatology simulation, based on the 5-member ensemble of WRF simulations.

were the main factor driving the Atlantic TC response to ENSO, with secondary contributions from midtropospheric RH.

c. Influence of mean climate change on Atlantic TCs

Before comparing the Atlantic TC response in each ENSO experiment between the future and historical climates, we analyzed the difference between the two climate states to try to separate the influences of mean climate change and changes in the ENSO teleconnection on Atlantic TCs. We found that mean-state climate change produces a decrease in future Atlantic TCs. The ensemble of future climatology simulations produced 14.8 Atlantic TCs per season, representing a 26% decrease from the 20 TCs per season in the historical climatology simulation (Tables 4 and 5 and Fig. 9a). We next investigated the connection between the TC response and large-scale environment and found a future decrease of 1%–2% in 700-hPa RH over most of the Atlantic TC genesis region (Fig. 8c) and an increase of 1–5 m s^{-1} in VWS (Figs. 8b,d) over the Atlantic TC genesis region. These thermodynamic and dynamic

changes make sense given the future change in mean-state SST toward more El Niño–like conditions (Fig. 8a) that support a future decrease in Atlantic TC activity. The 1–5 m s^{-1} future increase in VWS brought the ASO average VWS over the TC genesis region from 0 to 10 m s^{-1} for the historical to 2.5–15 m s^{-1} in the future (not shown). This indicates that the future mean climate state has the potential to strongly influence future changes in Atlantic TCs during El Niño, given the future increase in VWS and decrease in RH.

While Atlantic TC frequency decreased substantially in the future climatological simulation relative to the historical, seasonal Atlantic ACE decreased by a relatively moderate amount. The future simulations produced a 7% decrease in the ACE (Table 4 and Fig. 9b) or an ensemble average of 113 × 10^4 kt^2 in the future compared to 121 × 10^4 kt^2 in the historical (Table 5). Furthermore, the average ACE per TC increased by 26% in the future relative to the historical (Table 4). An increase in the ACE per TC means that, on average, the TCs live longer and/or are more intense. We found more long-track

TABLE 4. Change in Atlantic TC activity due to mean climate change for each given ENSO state. The seasonal Atlantic number of TCs and ACE (10^4 kt^2), represented as the percentage change, calculated as (future − historical)/historical, from each 5-member ensemble mean of the WRF TCM experiments with prescribed SST representing climatology, EP El Niño, CP El Niño, and La Niña. This represents the TC response to mean climate change for a given ENSO state.

	Climatology (%)	EP El Niño (%)	CP El Niño (%)	La Niña (%)
TCs per year	−26	−45	−20	−30
ACE per year	−7	−34	−5	−15
ACE per TC	26	19	18	21

TABLE 5. Seasonal Atlantic TC count and ACE (10^4 kt^2) from the 5-member ensemble mean of the WRF experiments with prescribed SST representing climatology, EP El Niño, CP El Niño, and La Niña in the historical and future climates. The percent change in each of the TC metrics for each ENSO experiment with respect to the corresponding climate's climatology is included in parentheses, which represents the TC response to ENSO for a given climate state. Standard deviation represents the variability between ensemble members.

	Climatology	EP El Niño	CP El Niño	La Niña
		Historical		
TCs per year	20	9 (−55%)	12.2 (−39%)	21.6 (8%)
ACE per year	120.6	50.4 (−58%)	67 (−44%)	134.1 (11%)
ACE per TC	6	5.6 (−7%)	5.5 (−10%)	6.2 (3%)
Standard deviation of TC count	3.9	1.8	0.8	3.4
Standard deviation of ACE	22.3	15.2	11.9	31.4
		Future		
TCs per year	14.8	5 (−66%)	9.8 (−34%)	15.2 (3%)
ACE per year	112.7	34 (−70%)	64.3 (−43%)	114.2 (1%)
ACE per TC	7.6	6.8 (−11%)	6.6 (−14%)	7.5 (−1%)
Standard deviation of TC count	2.3	1.8	2.6	2.6
Standard deviation of ACE	26.9	15.6	28.6	49.1

and stronger TCs in the future simulation compared to the historical, with a primary influence from increasing TC intensity. These findings align with other research (e.g., Bengtsson et al. 2007) on future increases in the TC intensity.

d. Influence of ENSO on Atlantic TCs in a future climate

The WRF TCM historical experiments demonstrated reasonable reliability in replicating the observed and simulated teleconnections between ENSO and Atlantic TC activity found in other research. In addition, the simulations have shown that if the CESM LENS is correct in predicting that the mean-state SSTs will become more El Niño–like in the future, there could be a future reduction of Atlantic TCs under neutral ENSO conditions. These findings make sense based on the current understanding of ENSO and Atlantic TCs. Now we investigate possible changes in the ENSO–Atlantic TC teleconnection under the more El Niño–like future mean climate state.

The first notable response in the future ENSO experiments is that each ENSO state experienced a substantial decrease in Atlantic TC frequency in the future relative to the historical (Table 5 and Figs. 5 and 9). This is most likely due to the mean state differences described in the previous section. Each ENSO simulation produced a decrease in Atlantic TCs and an increase in the ACE per TC in the future compared to the historical climate (Table 5 and Fig. 9). These results make sense, as the prescribed future decrease in the zonal tropical Pacific SST gradient shifts the mean state toward more El Niño–like conditions in the future, which in turn decreases Atlantic TC frequency in all experiments due to an average VWS increase and RH decrease (Fig. 4). Similarly, the intensity and longevity of the TCs increased in the future on average, which may be associated with warmer SSTs.

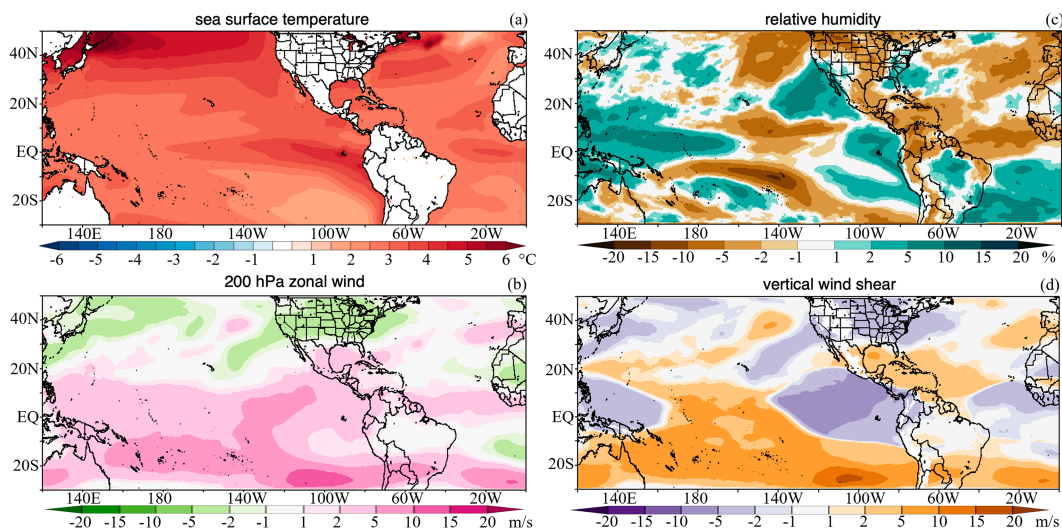Along with the mean decrease in the Atlantic TC frequency and increase in the TC intensity, the teleconnection ENSO

FIG. 8. Future change in the ASO averaged (a) SST (°C), (b) 200-hPa zonal winds (m s^{-1}), (c) 700-hPa RH (%), and (d) VWS (m s^{-1}) from the 5-member ensemble of the climatological future minus historical WRF simulations.
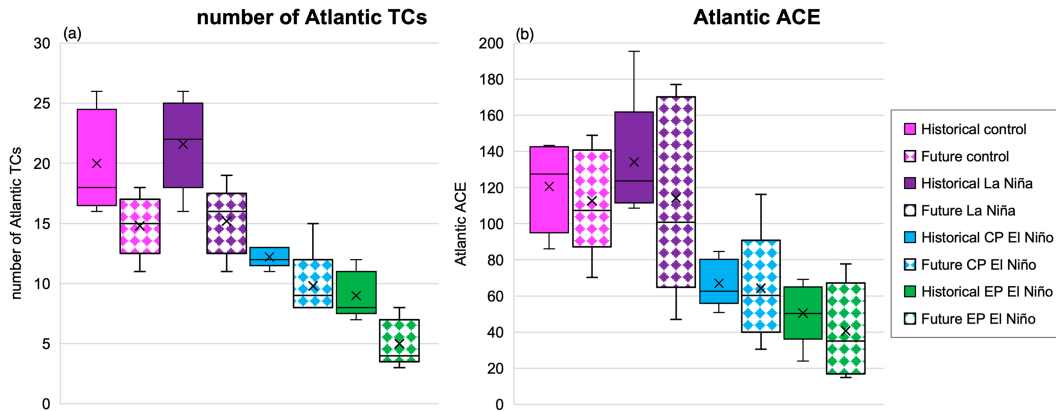
FIG. 9. Boxplots of the seasonal Atlantic (a) number of TCs and (b) ACE (10^4 kt^2) from the 5-member ensemble of each WRF experiment representing different ENSO states in historical and future climates.

currently has with Atlantic TC frequency remains relatively similar in the future (Table 5 and Fig. 10). Compared to each of their respective climate states (Table 5), the future EP El Niño still suppressed TCs (with a 66% and 55% decrease in the future and historical, respectively), the future CP El Niño still had a weaker TC suppression compared to EP El Niño (with a 34% and 39% decrease in the future and historical, respectively), and the future La Niña still slightly enhanced TC frequency (by 3% and 8% in the future and historical, respectively). Similar to the historical climate, the increase in the ensemble-mean number of TCs in the La Niña future simulation was less than one standard deviation above the ensemble-mean number of TCs in the control future simulation. The response in TC number to ENSO supports our finding that the location of tropical Pacific deep convection is a good indicator for ENSO's influence on Atlantic TCs in both the historical and future climates and that ENSO still impacts Atlantic VWS and 700-hPa RH (Figs. 6 and 7). Even with the ENSO–Atlantic TC teleconnection remaining similar in the future compared to the historical climate, it is worth noting that there were some relatively small differences. However, a larger

ensemble would be needed to determine whether the differences are significant or associated primarily with internal atmospheric variability.

So far, we have concluded that a future mean state change toward more El Niño–like conditions causes a general decrease in the Atlantic TC frequency, with a response in 200-hPa winds, VWS (driven mostly by changes in upper-tropospheric winds, rather than lower-tropospheric winds), and 700-hPa RH acting to reduce favorability for TCs. We have also determined that the ENSO–Atlantic TC teleconnection will be similar between the historical and future, with possible minor differences in strength. We now investigate whether the physical mechanisms that drive the teleconnection in the historical climate are also operating in the future climate.

The VWS responses to ENSO in the future mirrored those in the historical simulations (Fig. 6). For EP El Niño in both climates, there was a significant increase in the VWS of 10 m s^{-1} or more over the Atlantic TC genesis region (Figs. 6a,d). In addition, CP El Niño in both climates produced a VWS increase of around 2–5 m s^{-1} (Figs. 6b,e), again consistent with the Atlantic TC response. The La Niña experiments for both
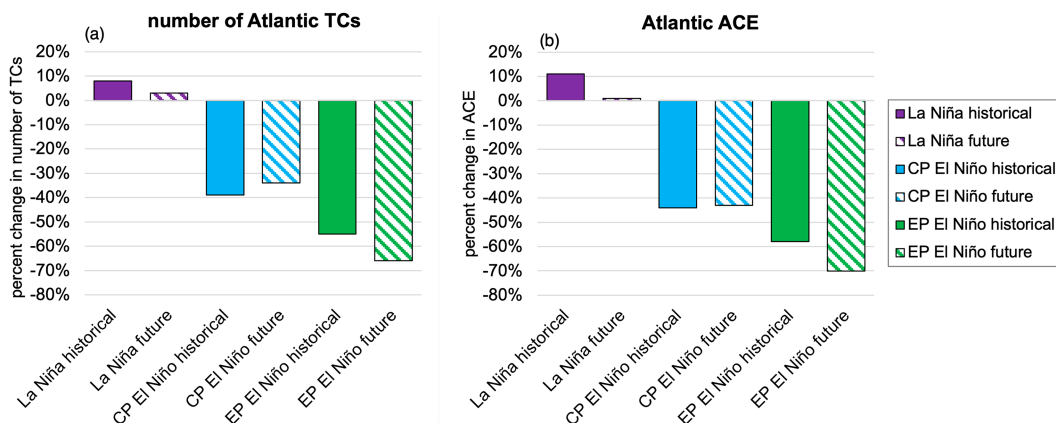

FIG. 10. Seasonal Atlantic (a) number of TCs and (b) ACE (10^4 kt^2) expressed as percentages relative to the respective climatology from the 5-member ensemble of WRF experiments representing different ENSO states in the historical and future climates.

climates produced a reduction in the VWS of up to 5 m s^{-1} over most of the TC genesis region (Figs. 6c,f). These teleconnections suggest that VWS is still highly correlated with the Atlantic 200-hPa zonal wind response to climate change (not shown) and therefore the extent to which zonal shifts in tropical Pacific deep convection impact VWS in the Atlantic.

The 700-hPa RH response to ENSO was relatively similar in the historical and future experiments (Fig. 7). EP and CP El Niño produced a 1%–5% reduction in RH over the Atlantic TC genesis region in both the historical and future climates. The small differences in the magnitude of the RH reduction between CP El Niño and EP El Niño once again indicate that VWS is the primary factor in the ENSO relationship with Atlantic TCs. La Niña produced a 1%–5% RH increase over the TC genesis region for both the future and historical climates.

Overall, ENSO has a similar influence on VWS and 700-hPa RH in the future compared to the historical climate, and the location of tropical Pacific deep convection continues to have important implications for the Atlantic TC response to ENSO, most notably by impacting the 200-hPa winds, which heavily influence VWS over the Atlantic. The response of VWS, 700-hPa RH, and the 200-hPa zonal winds in the historical and future simulations supports the conclusion that the influence of ENSO alone (i.e., without considering mean-state climate change) on Atlantic TCs will be relatively similar between the historical and future climates.

5. Discussion and conclusions

The teleconnection between ENSO and Atlantic TCs has historically provided a valuable source of seasonal TC predictability; however, it remains unknown how this teleconnection may change in the future in association with changes in both ENSO and the mean climate state. It is not guaranteed that the ENSO–TC teleconnection will remain the same as the climate changes, given that there are thresholds and nonlinearities in the climate system, for example, in the relationship between TCs and vertical wind shear. This research examines the importance of ENSO diversity and associated shifts in the Walker circulation on Atlantic TCs in the historical climate and how this relationship might change in a future climate. We used WRF tropical channel model simulations forced by SST patterns characteristic of the monthly varying climatology, eastern Pacific El Niño, central Pacific El Niño, and La Niña in historical and future climates. The SST patterns were derived from the CESM LENS simulations. The simulations were designed specifically to investigate changes in ENSO and the mean climate, and controlled for other factors important for Atlantic TC activity, such as Atlantic SST variability.

We first investigated how ENSO and the mean-state SST changed in the future in the CESM LENS. We found a future weakening of the zonal tropical Pacific SST gradient, which represents more El Niño–like mean state conditions, consistent with other studies (An et al. 2008; Cai et al. 2015; Fredriksen et al. 2020; Erickson and Patricola 2023). In addition, both El Niño and La Niña events during the peak Atlantic hurricane season became more frequent in the future in the CESM LENS.

We then evaluated the observed relationship between ENSO and Atlantic TCs and found that the WRF simulations were able to reasonably reproduce such relationships. The historical simulations showed that the location of tropical Pacific deep convection strongly influenced the frequency of Atlantic TCs during ENSO, with stronger Atlantic TC suppression the farther eastward the tropical Pacific deep convection was located. This relationship was generally seen in observations but is harder to quantify due to the short observational record combined with the influence of factors aside from ENSO, such as Atlantic SST variability, which were controlled for in our WRF experiments. Furthermore, the primary observed physical mechanisms for the ENSO–TC teleconnection were replicated well by the model, as vertical wind shear and relative humidity were both impacted by ENSO via zonal shifts in tropical Pacific deep convection. Of the two, vertical wind shear was the primary factor that drove the Atlantic TC frequency response to ENSO in our simulations.

We investigated the influence of ENSO on Atlantic TCs in a changing climate by first attempting to isolate the role of changes in the mean climate state. We found that future changes in the mean climate, including a weakening of the zonal tropical Pacific SST gradient, reduced Atlantic TC activity regardless of ENSO conditions. Under neutral ENSO conditions, the Atlantic TC frequency was reduced by 26% in the future relative to the historical. Future research investigating different possible future outcomes of ENSO and the zonal tropical Pacific SST gradient change (e.g., Seager et al. 2019; Sobel et al. 2023) would be useful to build upon this study, given the uncertainties in both. This could include simulations in which the tropical Pacific zonal SST gradient strengthened (became more La Niña–like), stayed the same, and weakened more strongly than in the CESM LENS (became even more El Niño–like). Since future ENSO projections are also uncertain, testing different future ENSO possibilities would improve our understanding, especially since the CESM LENS future trend to more El Niño–like conditions is not as strong as some other models represented in CMIP6 (Erickson and Patricola 2023).

Finally, the future simulations showed that the current ENSO–Atlantic TC relationship holds in the future and provided strong evidence for the continued importance of zonal shifts in tropical Pacific deep convection. In particular, we investigated the future ENSO teleconnection with Atlantic TCs and found it to be similar to that in the historical simulations. We found that in a future with a decreasing zonal tropical Pacific SST gradient, ENSO's influence on the Atlantic TC frequency will still strongly depend on zonal shifts in tropical Pacific deep convection. Atlantic TC frequency responded significantly to zonal shifts in tropical Pacific deep convection in the future, with El Niño suppressing TCs and La Niña enhancing them. Furthermore, the diversity in El Niño remained an important factor in the ENSO–Atlantic TC relationship, with eastern Pacific El Niño suppressing Atlantic TCs more strongly than central Pacific El Niño in the future climate simulations, as in the historical climate simulations. This suggests that the ENSO longitude index, which captures ENSO diversity and represents the tropical Pacific deep convection shifts that

determine ENSO's teleconnections with Atlantic TCs, will be useful in characterizing ENSO's influence on Atlantic TCs in future climates.

Even though the historical ENSO–Atlantic TC teleconnection was relatively similar in the future, we found slight differences in the magnitude that could be due to internal atmospheric variability. To determine whether there are significant differences in the future ENSO–TC teleconnection, a larger ensemble of TC-permitting simulations would be required. While additional ensemble members could not be performed in this study due to the computational costs, we note that five ensemble members were sufficient in determining the general future ENSO–TC relationship (Lee et al. 2021). To provide further support for the ensemble size, we tested whether a 5-member ensemble would be sufficient by randomly resampling five members of the 22-member ensemble of simulations forced by EP El Niño, CP El Niño, and the monthly varying climatological SST from Patricola et al. (2016). We performed the random resampling 1000 times and calculated the percent change in the Atlantic TC number in response to each EP El Niño and CP El Niño. Results from the resampling indicate that a 5-member ensemble is suitable for this type of study. Based on the full 22-member ensembles, the Atlantic TC number decreased in response to both EP El Niño and CP El Niño relative to the control simulation. When the data were resampled to a sample size of 5, only 3 out of the 1000 resamples (0.3%) produced an increase or no change in the Atlantic TC number for EP El Niño, and 46 of the 1000 resamples (4.6%) produced an increase or no change in the Atlantic TC number for CP El Niño. We highlight that the 5-member ensembles from this study produced a response in the Atlantic TC number to both EP and CP El Niño that is consistent with the response in the 22-member ensemble from Patricola et al. (2016).

In addition, it would be useful to investigate future ENSO–TC teleconnections using the suite of global model simulations that participated in CMIP6 in order to capture differences in future projections of ENSO. It would be a substantial computational expense to do so using a similar TC-permitting dynamical modeling methodology as in this study. However, such an investigation would be more feasible with statistical–dynamical models such as the Columbia Hazard model (CHAZ; Lee et al. 2018) and is planned for future work. Furthermore, it would be useful to perform additional dynamical model simulations, such as those performed in this study, forced with SST patterns from additional large-ensemble simulations including those from the Multi-Model Large Ensemble Archive (Deser et al. 2020). This would enable the investigation of how different future projections of both ENSO and the mean-state SST could impact the ENSO–Atlantic TC teleconnection in the future. Indeed, the importance of using both multimodel and large ensembles for future ENSO projection has been highlighted recently by Maher et al. (2023). Using 14 single-model initial-condition large ensembles, they demonstrated that different future changes in ENSO and the tropical Pacific arise from differences between the models, and not just internal variability. Such ENSO projections can be especially useful to provide estimates of future changes in the frequency of ENSO events. We note that our study investigated the future ENSO–Atlantic

TC teleconnection without making assumptions about future changes in the frequency of ENSO. Our simulations instead investigated the teleconnection given ENSO conditions in the historical and future climates. This approach provides useful information about the future ENSO–Atlantic TC teleconnection despite the uncertainty in the frequency of ENSO events in the future.

In conclusion, we found that although the ENSO–Atlantic TC relationship of the historical climate is maintained into the future, a future mean state change toward more El Niño–like conditions drove a substantial decrease (26%) in future Atlantic TC frequency. In addition, we found that the location of tropical Pacific deep convection, and its influence on tropical Atlantic vertical wind shear, remained the most important factor in ENSO's influence on Atlantic TCs in the future. This relationship emerged as one of the most important factors in determining whether the Atlantic TC frequency would increase or decrease in the future. How ENSO will change is one important factor in determining how the Atlantic TC frequency may change in the future, as further highlighted by this research. In attempting to reduce uncertainty in future projections of the Atlantic TC frequency, reliable projections of future changes in both ENSO and the zonal tropical Pacific SST gradient are among the leading factors to solving this complex problem.

REFERENCES

An, S.-I., J.-S. Kug, Y.-G. Ham, and I.-S. Kang, 2008: Successive modulation of ENSO to the future greenhouse warming. *J. Climate*, **21**, 3–21, https://doi.org/10.1175/2007JCLI1500.1.

Ashok, K., S. K. Behera, S. A. Rao, H. Weng, and T. Yamagata, 2007: El Niño Modoki and its possible teleconnection. *J. Geophys. Res.*, **112**, C11007, https://doi.org/10.1029/2006JC003798.

——, T. P. Sabin, P. Swapna, and R. G. Murtugudde, 2012: Is a global warming signature emerging in the tropical Pacific? *Geophys. Res. Lett.*, **39**, L02701, https://doi.org/10.1029/2011GL050232.

Bell, G. D., and M. Chelliah, 2006: Leading tropical modes associated with interannual and multidecadal fluctuations in North Atlantic hurricane activity. *J. Climate*, **19**, 590–612, https://doi.org/10.1175/JCLI3659.1.

——, and Coauthors, 2000: Climate assessment for 1999. *Bull. Amer. Meteor. Soc.*, **81**, S1–S50, https://doi.org/10.1175/1520-0477(2000)81[s1:CAF]2.0.CO;2.

Bengtsson, L., K. I. Hodges, M. Esch, N. Keenlyside, L. Kornblueh, J.-J. Luo, and T. Yamagata, 2007: How may tropical cyclones change in a warmer climate? *Tellus*, **59A**, 539–561, https://doi.org/10.1111/j.1600-0870.2007.00251.x.

Bjerknes, J., 1966: A possible response of the atmospheric Hadley circulation to equatorial anomalies of ocean temperature. *Tellus*, **18A**, 820–829, https://doi.org/10.3402/tellusa.v18i4.9712.

Bove, M. C., J. B. Eisner, C. W. Landsea, X. Niu, and J. J. O'Brien, 1998: Effect of El Niño on U.S. landfalling hurricanes, revisited. *Bull. Amer. Meteor. Soc.*, **79**, 2477–2482, https://doi.org/10.1175/1520-0477(1998)079<2477:EOENOO>2.0.CO;2.

Bullister, J. L., and M. J. Warner, 2015: Atmospheric Histories (1765–2015) for CFC-11, CFC-12, CFC-113, CCl$_4$, SF$_6$ and N$_2$O. NOAA National Centers for Environmental Information, accessed 29 March 2017, https://doi.org/10.3334/cdiac/otg.cfc_atm_hist_2015.

Cai, W., and Coauthors, 2015: Increased frequency of extreme La Niña events under greenhouse warming. *Nat. Climate Change*, **5**, 132–137, https://doi.org/10.1038/nclimate2492.

Camargo, S. J., 2013: Global and regional aspects of tropical cyclone activity in the CMIP5 models. *J. Climate*, **26**, 9880–9902, https://doi.org/10.1175/JCLI-D-12-00549.1.

——, A. G. Barnston, P. J. Klotzbach, and C. W. Landsea, 2007a: Seasonal tropical cyclone forecasts. *WMO Bull.*, **56**, 297–309.

——, K. A. Emanuel, and A. H. Sobel, 2007b: Use of a genesis potential index to diagnose ENSO effects on tropical cyclone genesis. *J. Climate*, **20**, 4819–4834, https://doi.org/10.1175/JCLI4282.1.

Capotondi, A., and Coauthors, 2015a: Understanding ENSO diversity. *Bull. Amer. Meteor. Soc.*, **96**, 921–938, https://doi.org/10.1175/BAMS-D-13-00117.1.

——, Y.-G. Ham, A. Wittenberg, and J.-S. Kug, 2015b: Climate model biases and El Niño Southern Oscillation (ENSO) simulation. US CLIVAR Variations, 5 pp., https://repository.library.noaa.gov/view/noaa/31041.

——, A. T. Wittenberg, J.-S. Kug, K. Takahashi, and M. J. McPhaden, 2020: ENSO diversity. *El Nino Southern Oscillation in a Changing Climate, Geophys. Monogr.*, Vol. 252, Amer. Geophys. Union, 65–86, https://doi.org/10.1002/9781119548164.ch4.

Chiang, J. C. H., and A. H. Sobel, 2002: Tropical tropospheric temperature variations caused by ENSO and their influence on the remote tropical climate. *J. Climate*, **15**, 2616–2631, https://doi.org/10.1175/1520-0442(2002)015<2616:TTTVCB>2.0.CO;2.

Collins, M., and Coauthors, 2010: The impact of global warming on the tropical Pacific Ocean and El Niño. *Nat. Geosci.*, **3**, 391–397, https://doi.org/10.1038/ngeo868.

Davis, C. A., 2018: Resolving tropical cyclone intensity in models. *Geophys. Res. Lett.*, **45**, 2082–2087, https://doi.org/10.1002/2017GL076966.

Deser, C., and Coauthors, 2020: Insights from Earth system model initial-condition large ensembles and future prospects. *Nat. Climate Change*, **10**, 277–286, https://doi.org/10.1038/s41558-020-0731-2.

Elsner, J. B., J. P. Kossin, and T. H. Jagger, 2008: The increasing intensity of the strongest tropical cyclones. *Nature*, **455**, 92–95, https://doi.org/10.1038/nature07234.

Erickson, N. E., and C. M. Patricola, 2023: Future projections of the El Niño—Southern Oscillation and tropical Pacific mean state in CMIP6. *J. Geophys. Res. Atmos.*, **128**, e2022JD037563, https://doi.org/10.1029/2022JD037563.

Fredriksen, H.-B., J. Berner, A. C. Subramanian, and A. Capotondi, 2020: How does El Niño–Southern Oscillation change under global warming—A first look at CMIP6. *Geophys. Res. Lett.*, **47**, e2020GL090640, https://doi.org/10.1029/2020GL090640.

Fu, D., P. Chang, C. M. Patricola, and R. Saravanan, 2019: High-resolution tropical channel model simulations of tropical cyclone climatology and intraseasonal-to-interannual variability. *J. Climate*, **32**, 7871–7895, https://doi.org/10.1175/JCLI-D-19-0130.1.

Garner, S. T., I. M. Held, T. Knutson, and J. Sirutis, 2009: The roles of wind shear and thermal stratification in past and projected changes of Atlantic tropical cyclone activity. *J. Climate*, **22**, 4723–4734, https://doi.org/10.1175/2009JCLI2930.1.

Goldenberg, S. B., and L. J. Shapiro, 1996: Physical mechanisms for the association of El Niño and West African rainfall with Atlantic major hurricane activity. *J. Climate*, **9**, 1169–1187, https://doi.org/10.1175/1520-0442(1996)009<1169:PMFTAO>2.0.CO;2.

——, C. W. Landsea, A. M. Mestas-Nunez, and W. M. Gray, 2001: The recent increase in Atlantic hurricane activity: Causes and implications. *Science*, **293**, 474–479, https://doi.org/10.1126/science.1060040.

Gray, W. M., 1984: Atlantic seasonal hurricane frequency. Part I: El Niño and 30 mb quasi-biennial oscillation influences. *Mon. Wea. Rev.*, **112**, 1649–1668, https://doi.org/10.1175/1520-0493(1984)112<1649:ASHFPI>2.0.CO;2.

Gualdi, S., E. Scoccimarro, and A. Navarra, 2007: Changes in tropical cyclone activity due to global warming: Results from a high-resolution coupled general circulation model. CMCC Research Paper 16, 41 pp., https://doi.org/10.2139/ssrn.1366806.

Hoerling, M. P., and A. Kumar, 2002: Atmospheric response patterns associated with tropical forcing. *J. Climate*, **15**, 2184–2203, https://doi.org/10.1175/1520-0442(2002)015<2184:ARPAWT>2.0.CO;2.

Horel, J. D., and J. M. Wallace, 1981: Planetary-scale atmospheric phenomena associated with the Southern Oscillation. *Mon. Wea. Rev.*, **109**, 813–829, https://doi.org/10.1175/1520-0493(1981)109<0813:PSAPAW>2.0.CO;2.

Hsu, W.-C., C. M. Patricola, and P. Chang, 2019: The impact of climate model sea surface temperature biases on tropical cyclone simulations. *Climate Dyn.*, **53**, 173–192, https://doi.org/10.1007/s00382-018-4577-5.

Huang, B., and Coauthors, 2017: Extended Reconstructed Sea Surface Temperature, version 5 (ERSSTv5): Upgrades, validations, and intercomparisons. *J. Climate*, **30**, 8179–8205, https://doi.org/10.1175/JCLI-D-16-0836.1.

Kalnay, E., and Coauthors, 1996: The NCEP/NCAR 40-Year Reanalysis Project. *Bull. Amer. Meteor. Soc.*, **77**, 437–472, https://doi.org/10.1175/1520-0477(1996)077<0437:TNYRP>2.0.CO;2.

Kanamitsu, M., W. Ebisuzaki, J. Woollen, S.-K. Yang, J. J. Hnilo, M. Fiorino, and G. L. Potter, 2002: NCEP–DOE AMIP-II Reanalysis (R-2). *Bull. Amer. Meteor. Soc.*, **83**, 1631–1644, https://doi.org/10.1175/BAMS-83-11-1631.

Kao, H.-Y., and J.-Y. Yu, 2009: Contrasting eastern-Pacific and central-Pacific types of ENSO. *J. Climate*, **22**, 615–632, https://doi.org/10.1175/2008JCLI2309.1.

Kay, J. E., and Coauthors, 2015: The Community Earth System Model (CESM) large ensemble project: A community resource for studying climate change in the presence of internal climate variability. *Bull. Amer. Meteor. Soc.*, **96**, 1333–1349, https://doi.org/10.1175/BAMS-D-13-00255.1.

Kim, S. T., and J.-Y. Yu, 2012: The two types of ENSO in CMIP5 models. *Geophys. Res. Lett.*, **39**, L11704, https://doi.org/10.1029/2012GL052006.

Klotzbach, P. J., 2011: The influence of El Niño–Southern Oscillation and the Atlantic multidecadal oscillation on Caribbean tropical cyclone activity. *J. Climate*, **24**, 721–731, https://doi.org/10.1175/2010JCLI3705.1.

——, M. A. Saunders, G. D. Bell, and E. S. Blake, 2017: North Atlantic seasonal hurricane prediction. *Climate Extremes: Patterns and Mechanisms*, *Geophys. Monogr.*, Vol. 226, Amer. Geophys. Union, 315–328, https://doi.org/10.1002/9781119068020.ch19.

——, and Coauthors, 2022: A hyperactive end to the Atlantic hurricane season October–November 2020. *Bull. Amer. Meteor. Soc.*, **103**, E110–E128, https://doi.org/10.1175/BAMS-D-20-0312.1.

Knapp, K. R., M. C. Kruk, D. H. Levinson, H. J. Diamond, and C. J. Neumann, 2010: The International Best Track Archive for Climate Stewardship (IBTrACS) unifying tropical cyclone data. *Bull. Amer. Meteor. Soc.*, **91**, 363–376, https://doi.org/10.1175/2009BAMS2755.1.

Knutson, T., C. Landsea, and K. Emanuel, 2010: Tropical cyclones and climate change: A review. *Global Perspectives on Tropical Cyclones: From Science to Mitigation*, J. C. L. Chan and J. D. Kepert, Eds., World Scientific Series on Asia-Pacific Weather and Climate, Vol. 4, World Scientific, 243–284, https://doi.org/10.1142/9789814293488_0009.

——, and Coauthors, 2019: Tropical cyclones and climate change assessment: Part I: Detection and attribution. *Bull. Amer. Meteor. Soc.*, **100**, 1987–2007, https://doi.org/10.1175/BAMS-D-18-0189.1.

——, and Coauthors, 2020: Tropical cyclones and climate change assessment: Part II: Projected response to anthropogenic warming. *Bull. Amer. Meteor. Soc.*, **101**, E303–E322, https://doi.org/10.1175/BAMS-D-18-0194.1.

Kug, J.-S., and Y.-G. Ham, 2011: Are there two types of La Nina? *Geophys. Res. Lett.*, **38**, L16704, https://doi.org/10.1029/2011GL048237.

——, F.-F. Jin, and S.-I. An, 2009: Two types of El Niño events: Cold tongue El Niño and warm pool El Niño. *J. Climate*, **22**, 1499–1515, https://doi.org/10.1175/2008JCLI2624.1.

——, Y.-G. Ham, J.-Y. Lee, and F.-F. Jin, 2012: Improved simulation of two types of El Niño in CMIP5 models. *Environ. Res. Lett.*, **7**, 034002, https://doi.org/10.1088/1748-9326/7/3/034002.

Landsea, C. W., and J. L. Franklin, 2013: Atlantic hurricane database uncertainty and presentation of a new database format. *Mon. Wea. Rev.*, **141**, 3576–3592, https://doi.org/10.1175/MWR-D-12-00254.1.

——, R. A. Pielke Jr., A. M. Mestas-Nuñez, and J. A. Knaff, 1999: Atlantic basin hurricanes: Indices of climatic changes. *Weather Climate Extreme*, T. R. Karl, N. Nicholls, and A. Ghazi, Eds., Springer, 89–129, https://doi.org/10.1007/978-94-015-9265-9_9.

Lee, C.-Y., M. K. Tippett, A. H. Sobel, and S. J. Camargo, 2018: An environmentally forced tropical cyclone hazard model. *J. Adv. Model. Earth Syst.*, **10**, 223–241, https://doi.org/10.1002/2017MS001186.

Lee, J., Y. Y. Planton, P. J. Gleckler, K. R. Sperber, E. Guilyardi, A. T. Wittenberg, M. J. McPhaden, and G. Pallotta, 2021: Robust evaluation of ENSO in climate models: How many ensemble members are needed? *Geophys. Res. Lett.*, **48**, e2021GL095041, https://doi.org/10.1029/2021GL095041.

Lee, S., M. L'Heureux, A. T. Wittenberg, R. Seager, P. A. O'Gorman, and N. C. Johnson, 2022: On the future zonal contrasts of equatorial Pacific climate: Perspectives from observations, simulations, and theories. *npj Climate Atmos. Sci.*, **5**, 82, https://doi.org/10.1038/s41612-022-00301-2.

Lee, T., and M. J. McPhaden, 2010: Increasing intensity of El Niño in the central-equatorial Pacific. *Geophys. Res. Lett.*, **37**, L14603, https://doi.org/10.1029/2010GL044007.

Lin, I.-I., and Coauthors, 2020: ENSO and tropical cyclones. *El Niño Southern Oscillation in a Changing Climate*, *Geophys. Monogr.*, Vol. 253, Amer. Geophys. Union, 377–408, https://doi.org/10.1002/9781119548164.ch17.

Maher, N., D. Matei, S. Milinski, and J. Marotzke, 2018: ENSO change in climate projections: Forced response or internal variability? *Geophys. Res. Lett.*, **45**, 11 390–11 398, https://doi.org/10.1029/2018GL079764.

——, and Coauthors, 2023: The future of the El Niño–Southern Oscillation: Using large ensembles to illuminate time-varying responses and inter-model differences. *Earth Syst. Dyn.*, **14**, 413–431, https://doi.org/10.5194/esd-14-413-2023.

NOAA NCEI, 2024: U.S. billion-dollar weather and climate disasters, 1980–present. NOAA National Centers for Environmental Information, accessed 31 March 2024, https://doi.org/10.25921/stkw-7w73.

Patricola, C. M., R. Saravanan, and P. Chang, 2014: The impact of the El Niño–Southern Oscillation and Atlantic meridional mode on seasonal Atlantic tropical cyclone activity. *J. Climate*, **27**, 5311–5328, https://doi.org/10.1175/JCLI-D-13-00687.1.

——, P. Chang, and R. Saravanan, 2016: Degree of simulated suppression of Atlantic tropical cyclones modulated by flavour of El Niño. *Nat. Geosci.*, **9**, 155–160, https://doi.org/10.1038/ngeo2624.

Pielke, R. A., Jr., and C. N. Landsea, 1999: La Nina, El Nino, and Atlantic hurricane damages in the United States. *Bull. Amer. Meteor. Soc.*, **80**, 2027–2034, https://doi.org/10.1175/1520-0477(1999)080<2027:LNAENO>2.0.CO;2.

——, C. Landsea, M. Mayfield, J. Layer, and R. Pasch, 2005: Hurricanes and global warming. *Bull. Amer. Meteor. Soc.*, **86**, 1571–1576, https://doi.org/10.1175/BAMS-86-11-1571.

Ren, H.-L., and F.-F. Jin, 2011: Niño indices for two types of ENSO. *Geophys. Res. Lett.*, **38**, L04704, https://doi.org/10.1029/2010GL046031.

Riahi, K., and Coauthors, 2011: RCP 8.5—A scenario of comparatively high greenhouse gas emissions. *Climatic Change*, **109**, 33, https://doi.org/10.1007/s10584-011-0149-y.

Richter, I., 2015: Climate model biases in the eastern tropical oceans: Causes, impacts and ways forward. *Wiley Interdisc. Rev.: Climate Change*, **6**, 345–358, https://doi.org/10.1002/wcc.338.

Rios-Berrios, R., and R. D. Torn, 2017: Climatological analysis of tropical cyclone intensity changes under moderate vertical

wind shear. *Mon. Wea. Rev.*, **145**, 1717–1738, https://doi.org/10.1175/MWR-D-16-0350.1.

Schär, C., C. Frei, D. Lüthi, and H. C. Davies, 1996: Surrogate climate-change scenarios for regional climate models. *Geophys. Res. Lett.*, **23**, 669–672, https://doi.org/10.1029/96GL00265.

Seager, R., M. Cane, N. Henderson, D.-E. Lee, R. Abernathey, and H. Zhang, 2019: Strengthening tropical Pacific zonal sea surface temperature gradient consistent with rising greenhouse gases. *Nat. Climate Change*, **9**, 517–522, https://doi.org/10.1038/s41558-019-0505-x.

Skamarock, W. C., and Coauthors, 2019: A description of the Advanced Research WRF Model version 4. NCAR Tech. Note NCAR/TN-556+STR, 145 pp., https://doi.org/10.5065/1dfh-6p97.

Smith, A. B., 2022: 2021 U.S. billion dollar weather and climate disasters in historical context including new county-level exposure, vulnerability and projected damage mapping. *Major Weather Events and Impacts of 2021*, Houston, TX, Amer. Meteor. Soc., 5.3, https://ams.confex.com/ams/102ANNUAL/meetingapp.cgi/Paper/389010.

Smith, S. R., J. Brolley, J. J. O'Brien, and C. A. Tartaglione, 2007: ENSO's impact on regional U.S. hurricane activity. *J. Climate*, **20**, 1404–1414, https://doi.org/10.1175/JCLI4063.1.

Sobel, A. H., A. A. Wing, S. J. Camargo, C. M. Patricola, G. A. Vecchi, C.-Y. Lee, and M. K. Tippett, 2021: Tropical cyclone frequency. *Earth's Future*, **9**, e2021EF002275, https://doi.org/10.1029/2021EF002275.

——, and Coauthors, 2023: Near-term tropical cyclone risk and coupled Earth system model biases. *Proc. Natl. Acad. Sci. USA*, **120**, e2209631120, https://doi.org/10.1073/pnas.2209631120.

Stevenson, S. L., 2012: Significant changes to ENSO strength and impacts in the twenty-first century: Results from CMIP5. *Geophys. Res. Lett.*, **39**, L17703, https://doi.org/10.1029/2012GL052759.

Tang, B. H., and J. D. Neelin, 2004: ENSO Influence on Atlantic hurricanes via tropospheric warming. *Geophys. Res. Lett.*, **31**, L24204, https://doi.org/10.1029/2004GL021072.

Tang, T., J.-J. Luo, K. Peng, L. Qi, and S. Tang, 2021: Over-projected Pacific warming and extreme El Niño frequency due to CMIP5 common biases. *Natl. Sci. Rev.*, **8**, nwab056, https://doi.org/10.1093/nsr/nwab056.

Tao, D., and F. Zhang, 2014: Effect of environmental shear, sea-surface temperature, and ambient moisture on the formation and predictability of tropical cyclones: An ensemble-mean perspective. *J. Adv. Model. Earth Syst.*, **6**, 384–404, https://doi.org/10.1002/2014MS000314.

——, and ——, 2015: Effects of vertical wind shear on the predictability of tropical cyclones: Practical versus intrinsic limit. *J. Adv. Model. Earth Syst.*, **7**, 1534–1553, https://doi.org/10.1002/2015MS000474.

Timmermann, A., and Coauthors, 2018: El Niño–Southern Oscillation complexity. *Nature*, **559**, 535–545, https://doi.org/10.1038/s41586-018-0252-6.

Tsutsumi, Y., K. Mori, T. Hirahara, M. Ikegami, and T. J. Conway, 2009: Technical report of global analysis method for major greenhouse gasses by the world data center for greenhouse gasses. GAW Rep. 184, 31 pp., https://www.wmo.int/pages/prog/arep/gaw/documents/TD_1473_GAW184_web.pdf.

Vecchi, G. A., and T. R. Knutson, 2008: On estimates of historical North Atlantic tropical cyclone activity. *J. Climate*, **21**, 3580–3600, https://doi.org/10.1175/2008JCLI2178.1.

——, and ——, 2011: Estimating annual numbers of Atlantic hurricanes missing from the HURDAT database (1878–1965) using ship track density. *J. Climate*, **24**, 1736–1746, https://doi.org/10.1175/2010JCLI3810.1.

——, C. Landsea, W. Zhang, G. Villarini, and T. Knutson, 2021: Changes in Atlantic major hurricane frequency since the late-19th century. *Nat. Commun.*, **12**, 4054, https://doi.org/10.1038/s41467-021-24268-5.

Walsh, K., 1997: Objective detection of tropical cyclones in high-resolution analyses. *Mon. Wea. Rev.*, **125**, 1767–1779, https://doi.org/10.1175/1520-0493(1997)125<1767:ODOTCI>2.0.CO;2.

Walsh, K. J. E., and Coauthors, 2016: Tropical cyclones and climate change. *Wiley Interdiscip. Rev.: Climate Change*, **7**, 65–89, https://doi.org/10.1002/wcc.371.

Williams, I. N., and C. M. Patricola, 2018: Diversity of ENSO events unified by convective threshold sea surface temperature: A nonlinear ENSO index. *Geophys. Res. Lett.*, **45**, 9236–9244, https://doi.org/10.1029/2018GL079203.

Yeh, S.-W., J.-S. Kug, B. Dewitte, M.-H. Kwon, B. P. Kirtman, and F.-F. Jin, 2009: El Niño in a changing climate. *Nature*, **461**, 511–514, https://doi.org/10.1038/nature08316.

——, ——, and S.-I. An, 2014: Recent progress on two types of El Niño: Observations, dynamics, and future changes. *Asia-Pac. J. Atmos. Sci.*, **50**, 69–81, https://doi.org/10.1007/s13143-014-0028-3.

Yu, J., Y. Wang, and K. Hamilton, 2010: Response of tropical cyclone potential intensity to a global warming scenario in the IPCC AR4 CGCMs. *J. Climate*, **23**, 1354–1373, https://doi.org/10.1175/2009JCLI2843.1.

Zhang, F., and D. Tao, 2013: Effects of vertical wind shear on the predictability of tropical cyclones. *J. Atmos. Sci.*, **70**, 975–983, https://doi.org/10.1175/JAS-D-12-0133.1.

Zhao, M., and I. M. Held, 2010: An analysis of the effect of global warming on the intensity of Atlantic hurricanes using a GCM with statistical refinement. *J. Climate*, **23**, 6382–6393, https://doi.org/10.1175/2010JCLI3837.1.

Zhao, X., and R. J. Allen, 2019: Strengthening of the walker circulation in recent decades and the role of natural sea surface temperature variability. *Environ. Res. Commun.*, **1**, 021003, https://doi.org/10.1088/2515-7620/ab0dab.

Zheng, X.-T., S.-P. Xie, L.-H. Lv, and Z.-Q. Zhou, 2016: Intermodel uncertainty in ENSO amplitude change tied to Pacific Ocean warming pattern. *J. Climate*, **29**, 7265–7279, https://doi.org/10.1175/JCLI-D-16-0039.1.

——, C. Hui, and S.-W. Yeh, 2018: Response of ENSO amplitude to global warming in CESM large ensemble: Uncertainty due to internal variability. *Climate Dyn.*, **50**, 4019–4035, https://doi.org/10.1007/s00382-017-3859-7.

Zuidema, P., and Coauthors, 2016: Challenges and prospects for reducing coupled climate model SST biases in the eastern tropical Atlantic and Pacific Oceans: The U.S. CLIVAR eastern tropical oceans synthesis working group. *Bull. Amer. Meteor. Soc.*, **97**, 2305–2328, https://doi.org/10.1175/BAMS-D-15-00274.1.